Contrib Mineral Petrol (2001) 140: 567–576
DOI 10.1007/s004100000200

Johannes Duyster · Bernhard Stöckhert

Grain boundary energies in olivine derived from natural microstructures

Received: 26 May 2000 / Accepted: 12 September 2000 / Published online: 31 October 2000

Abstract An absolute value for the interfacial free energy of high-angle grain boundaries in olivine/fo_{90} has been derived from a microstructurally equilibrated coarse-grained natural peridotite. The three-dimensional configuration of high and low-angle grain boundaries and the disorientation were determined simultaneously in transmitted light with a universal stage on a polarizing microscope. For the low-angle grain boundaries, the interfacial free energy was calculated for the dislocation configuration indicated by the disorientation, using the model of Read and Shockley (Phys Rev 78(3):275–289, 1950). A dislocation core radius of 1/2b (b = magnitude of the Burgers vector) is suggested by fitting the theoretical function to the plot of relative grain boundary energy versus disorientation. The relative grain boundary energy is obtained from the dihedral angle at grain edges. Torque forces can be neglected because high-angle grain boundaries are not facetted and low-angle grain boundaries are unilaterally rational tilt boundaries parallel to (100) with a rotation axis parallel [001]. The relation between sub-grain disorientation and dihedral angles at grain edges yields an absolute value for the energy of high-angle grain boundaries of $\sim$1.4 J m^{-2}. The advantages of using natural materials are that (1) experimental efforts are minimal, (2) the material is coarse grained and thus three-dimensional grain boundary configuration and crystallographic orientation can both be studied simultaneously in transmitted light, (3) the low energy grain boundary configuration was adjusted over geological time scales in the solid state, and (4) effects of impurities on grain boundary energies and mobilities are those relevant to natural conditions.

Key words Grain-boundary energies · Interfacial free energies · Microstructures · Olivine

J. Duyster (✉) · B. Stöckhert
Institut für Geologie, Mineralogie und Geophysik,
Ruhr-Universität, 44780 Bochum, Germany
E-mail: johannes.duyster@ruhr-uni-bochum.de

Introduction

The free energy associated with grain boundaries, interphase boundaries and surfaces referred here as interfacial free energies (IFE), is in the order of 1 J m^{-2} for many crystalline materials (Sutton and Baluffi 1996). It represents a very small contribution to the total free energy of a system compared with other factors, for example, the elastic strain energy arising from the presence of dislocations, which is typically about two to four orders of magnitude higher. Nevertheless, IFE control fundamental processes and properties such as nucleation, grain growth, grain shape, and the geometry – and thus mobility – of intergranular fluids and melts, provided the other energy terms, such as chemical free energies and differences in plastic and elastic strain energies across the interfaces, are minimized and temperatures are sufficiently high to allow adjustment of a low energy interface configuration. Grain shape and the geometry of second phase distribution, controlled by the relative magnitude of IFE (Voll 1960; Kretz 1966, 1969; Spry 1969; Vernon 1976), is conveniently described by specification of dihedral angles (Smith 1964). In turn, dihedral angles also serve to derive relative magnitudes of IFE. Data for many metals and alloys, and for some minerals, have been experimentally determined (Murr 1975).

For olivine, IFEs are of special interest because they control the interconnectivity of melt in the upper mantle, governing both the extraction of basalt from peridotite and mantle rheological properties. The dihedral angles for basaltic melt in polycrystalline olivine were experimentally determined by – among others – Bulau et al. (1979), Waff and Bulau (1979), Cooper and Kohlstedt (1982), Waff and Bulau (1982), Turamori and Fujii (1986) and recently by Cmiral et al. (1998) and Jung and Waff (1998). Cooper and Kohlstedt (1982) carried out thermal etching and melting experiments on single crystal olivine as well as on synthetic peridotite samples. They reported scalar values for grain and in-

terphase boundary energies in the system, derived from dihedral angles. From the ratio of the low-angle grain boundary energy to the energy of the solid liquid interface they calculated the energy of the latter and then, using a dihedral angle between high-angle grain boundaries and melt reported by Waff and Bulau (1979), they calculated the energy of high-angle grain boundaries.

Their approach is based on two prerequisites: the free energies are independent of crystallographic orientation, and the free energies of low-angle grain boundaries can be computed applying linear elastic theory.

Other studies have shown, however, that the phase boundaries between olivine and melt tend to be faceted and that rational interfaces (with low Miller indices) predominate (t'Hart 1978a,b; Waff and Faul 1992; Cmiral et al. 1998; Jung and Waff 1998). Apart from the pioneering study by Cooper and Kohlstedt (1982), to our knowledge, no independent determinations of absolute values for the grain boundary energies of olivine have been reported.

In the present study, we have attempted to determine the absolute value of the high-angle grain boundary energy of olivine from dihedral angles at grain edges, where one low and two high-angle grain boundaries meet, in a natural peridotite. The use of natural material minimizes the usual experimental uncertainties related to whether time was sufficient to reach mechanical equilibrium, and to the influence of impurities. More important, in the coarse-grained material the true interface configuration in three dimensions can be investigated, using transmitted light, together with the relative crystallographic orientation of the grains at the same microstructural site.

Geological setting and description of the specimen

The mafic-ultramafic complex of Finero is a kilometer-sized, lens-shaped body at the base of the Ivrea Zone (Zingg 1983), Western Alps. The ultramafic suite is composed of layered cumulates in contact with a phlogopite bearing mantle peridotite (Coltorti and Siena 1984; Lu et al. 1997a,b; Zanetti et al. 1999). Descriptions of the structures and microstructures are found in Lensch (1968) and Kruhl and Voll (1979).

Our specimen is a phlogopite-bearing mantle peridotite. It is made up of ~85% of millimeter-sized olivine grains: 10% orthopyroxene and up to 5% of phlogopite and opaque minerals. The refractive indices of large olivine grains, determined by spindle stage, are: $nx = 1.6529$, $ny = 1.6702$, $nz = 1.6876$ (± 0.001), with an angle $2Vz = 87°$. The fayalite mole fraction indicated by these optical properties is ~0.1.

Two principal stages of microstructural evolution are discernible: An earlier stage is represented by millimeter-sized olivine grains with straight or smoothly curved high-angle grain boundaries. These large olivine grains show evidence of annealing after slight inhomogeneous deformation by dislocation creep. Geometrically necessary dislocations are arranged into sub-grain boundaries, most of which are sub-parallel to each other (Fig 1a, b, d). In these coarse-grained domains, the configuration of low and high-angle grain boundaries (LAGB and HAGB) reflects the relative magnitudes of the grain boundary energies. A later stage of ductile deformation in the peridotite is localized along shear zones. There, olivine is recrystallized dynamically with a

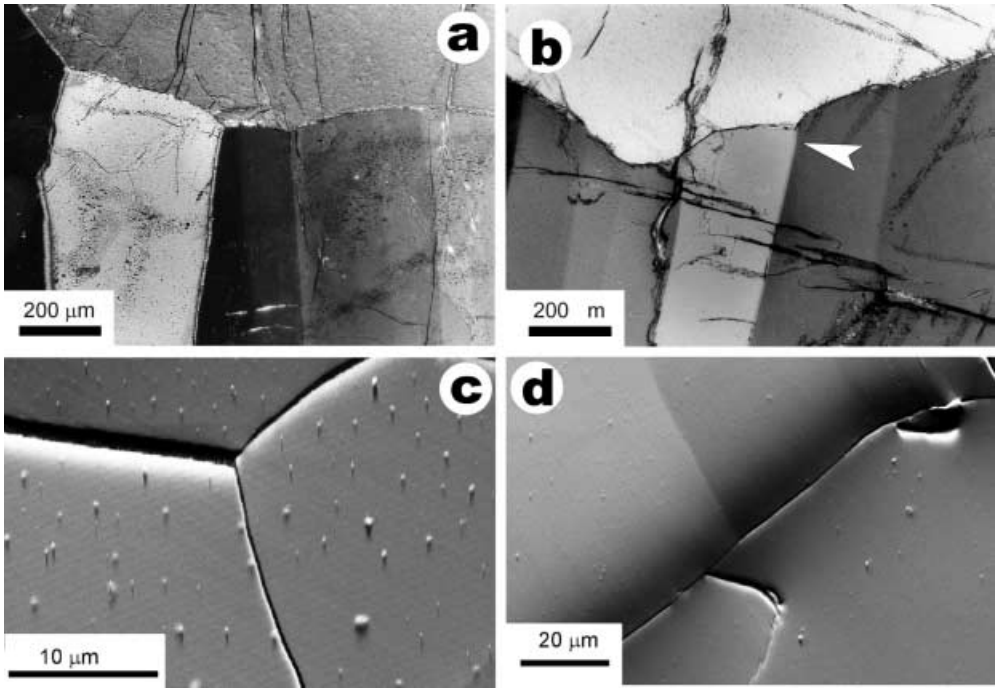

Fig. 1 Olivine sub-grain boundaries meeting high-angle grain boundaries at triple junctions. **a–b** Optical micrographs, crossed polarizers. *Arrow* in image **b** points to kink in sub-grain boundary (see Fig. 2b). **c–d** Orientation contrast (forward-scattered electron) SEM images

grain size of ~50 μm and below. The grain boundaries are sutured and the grains reveal undulatory extinction. Our study is concerned with the coarse-grained domains where the earlier microstructural record is not visibly affected by the later overprint.

Methods

In our study, the grain boundary configuration and relative crystallographic orientation of the olivine grains were determined in transmitted light using a polarizing microscope equipped with a universal stage. This approach has the significant advantage that the 3D geometry of the grain boundary configuration and the relative crystallographic orientation of the three grains can be studied simultaneously, which is not possible with electron backscatter diffraction (EBSD) in a scanning electron microscope (SEM), mainly because of the lack of appropriate access to the third dimension. TEM studies allow limited 3D access, but are restricted to very fine-grained material.

A coarse-grained sample of peridotite was cut into 30 slices and a thin section of 0.04 mm thickness, polished on both sides, was prepared from each slice.

Suitable sites in the olivine microstructure had to obey the following criteria:

- A LAGB (sub-grain boundary) meets two HAGBs.
- The grains show no undulatory extinction, i.e., geometrically necessary dislocations are concentrated in the LAGB.
- The grain boundaries are planar or smoothly curved, not faceted, and do not show any indication of strain-induced boundary migration.
- The inclination of the boundaries with respect to the section plane is steep enough that their orientation can be measured by universal stage.

Around 50 sites within the 30 examined thin sections fulfilled all these criteria and were accordingly selected for analysis.

First, the disorientation of the three grains and sub-grains, respectively, was determined. The disorientation between two sub-grains is defined as the angle of rotation required to get the lattices into an identical orientation. A rotation is described by specifying the rotation axis (two angles) and the angle of rotation (one angle). In crystals with symmetry elements, other than identity, more than one rotation can be defined according to the above definition. In this case, the disorientation angle is defined as the smallest rotation angle of the set. The uncertainty of the crystallographic orientation determined with the universal stage is normally ~1°, or at most 2°, depending on the orientation of the crystal with respect to the thin section. We tried to optimize the results in the following way. The orientation of two principal axes of the indicatrix was measured for every crystal, and – wherever possible – this was done for all three axes. Only data sets indicating angles $>89°$ between the principal axes were accepted. Given the orthorhombic symmetry of olivine, the Euler angles are readily determined for each crystal from the indicatrix orientation. To check the precision of the determination of the crystallographic orientations with the universal stage we have additionally performed EBSD measurements on selected sites. In general, EBSD measurements provide slightly more precise results with errors in the range of ± 0.5–1°. Our EBSD data are in very good agreement with the universal stage measurements. A comparison of EBSD and universal stage data is displayed in Fig. 2a.

Second, the orientation of the grain boundaries was determined. This was done by measuring the orientation of a tangential plane on the boundary, which contains the grain edge. The intersection of this tangential plane with the plane of the thin section (the azimuth or "strike") can be determined with an error of $<1°$. However, the error with respect to the inclination of the boundary (the "dip") is somewhat larger, in particular in the case of LAGBs. The results were reproducible by repeated measurements to within ~2°. If the boundaries are planar or simply curved around an axis parallel to the intersection direction then the correctly determined traces of three grain-boundaries meeting at a grain edge should intersect at one point in the stereographic projection (Fig. 2a, b). In most cases this requirement was met with a deviation of less than a few degrees. Only these results were accepted. In cases where the compatibility requirement was not met, repetition of the measurements showed that the failure did generally not result from inaccuracy, but rather from the fact that the boundaries were not strictly planar or simply curved. In these cases the grain boundary configuration is possibly influenced by microstructural features (grain edges, interphase boundaries, inclusions, etc.) beyond the volume of the thin section, which are thus no longer accessible. Altogether, 25 high-quality data sets for the configuration at grain edges were gathered. Additionally, some high-angle grain boundaries have been included for comparison.

Derivation of grain boundary energies from microstructures

Interfacial free energy and grain boundary configuration – theoretical background

Grain boundaries separate domains of the same crystal species with contrasting orientation. Depending on the angle of disorientation (Sutton and Baluffi 1996), low-angle grain boundaries (LAGBs) separate sub-grains and are distinguished from high-angle grain boundaries (HAGBs). At grain boundaries, the crystal structure is distorted and atoms are deprived of some of their neighbors. The lattice strain resulting from this disorder and the broken bonds contribute to the free energy of a volume of material. In order to minimize the free energy a system attempts to reduce its total area of grain boundaries, with interfacial tension being the driving force. The result is a grain boundary configuration with planar to slightly curved (because of space-filling requirements; Underwood 1970) grain boundaries. In "mechanical equilibrium", the angles at the grain edges reflect the balance of forces associated with the respective grain boundary tensions (Smith 1964). If the grain boundary energy does not depend on the orientation with respect to the lattice, the relative magnitudes of the interfacial tensions can be deduced from the geometry of such low energy grain boundary configurations. For mechanical equilibrium, the so-called dihedral angles reflect the relative magnitudes of the interfacial tensions according to the relationship

$$\frac{\gamma_g(1)}{\sin\alpha_1} = \frac{\gamma_g(2)}{\sin\alpha_2} = \frac{\gamma_g(3)}{\sin\alpha_3} \quad (1)$$

where $\gamma_g(1)$, $\gamma_g(2)$ and $\gamma_g(3)$ are the interfacial energies of the grain boundaries meeting at the grain edge, and α_1, α_2 and α_3 are the dihedral angles (Fig. 3; Smith 1964). In the simplest case, when the energies of the three boundaries are equal, the equilibrium configuration is characterized by dihedral angles of 120°.

LAGBs are semi-coherent boundaries and composed of a regular array of dislocations (Kelly and Groves 1970). As the number of the geometrically necessary

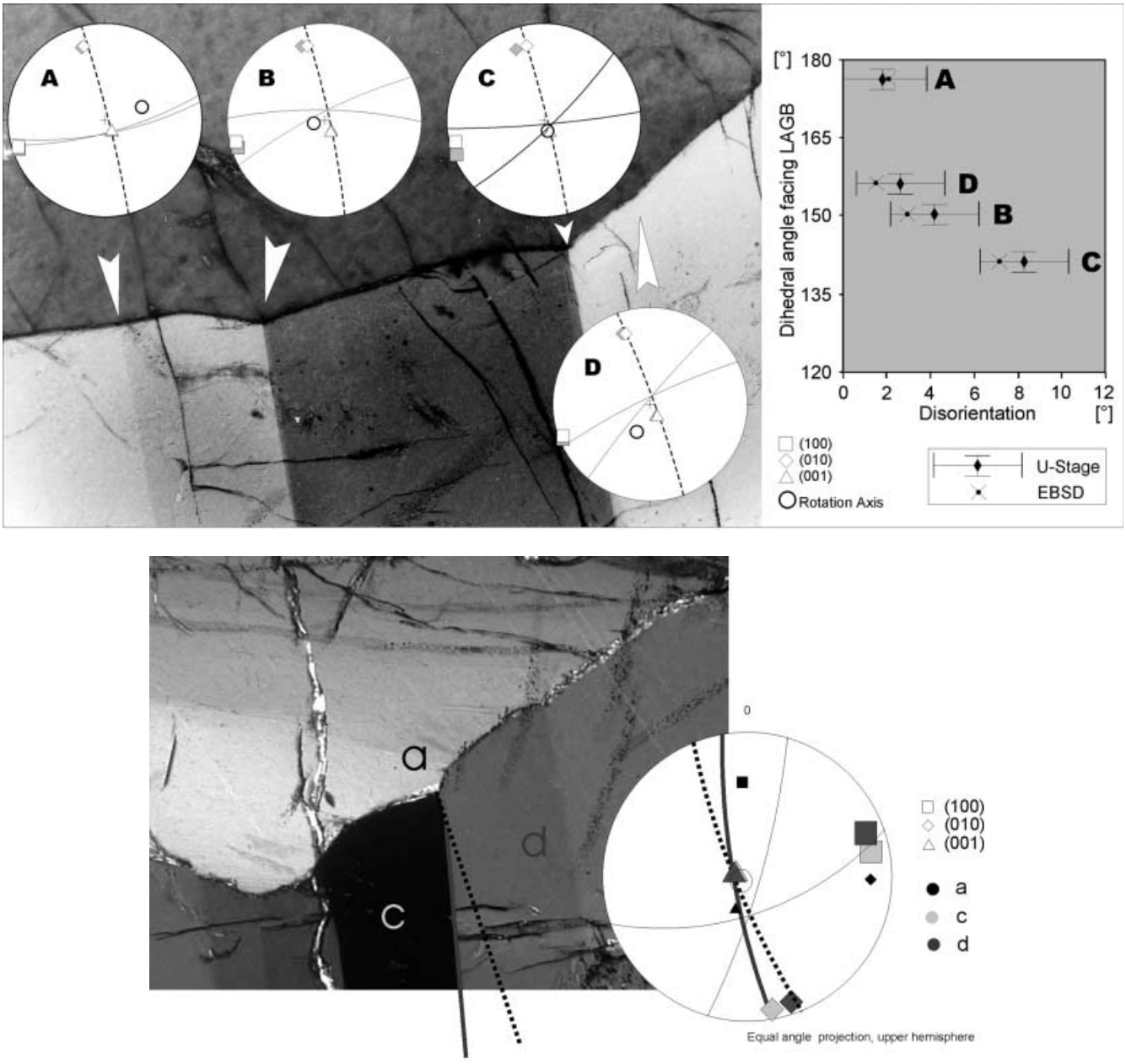

Fig. 2 *a* Sub-grain boundaries unilaterally rational, parallel to (100). The dihedral angles facing the sub-grains decrease with increasing disorientation. The rotation axes of the disorientation are near [001]. Note that the determination of rotation axes is more precise for larger disorientations. All stereographic projections are equal-angle, upper hemisphere projections. *Great circles* indicate interface orientations, LAGB are *stippled*. *b* Olivine grain with unilaterally rational sub-grain boundaries parallel to (100). The direction of [001] in grain a and d is perpendicular to the section plane. Disorientation between grain *a* and *d* is 9°. *Open circle* in stereographic projection indicates orientation of the rotation axis which is parallel to [001]. Note the kink in the sub-grain boundary between grain *a* and *d*. Below the kink, the boundary is unilaterally rational with respect to grain *a*; above the kink it is rational with respect to grain *b*. In the stereographic projection the upper part of the interface *a–d* (*stippled*), and the interfaces *a–b* and *b–d* intersect very close to each other

dislocations in the boundary increases with increasing disorientation, the same is true for the IFE of LAGBs. In contrast, HAGBS are generally non-coherent and their energies are independent of disorientation, apart from some special orientations (Sutton and Baluffi 1996). Therefore, at grain edges where two HAGBs meet a LAGB, the energies of the two HAGBs are likely to be approximately identical. If none of the boundaries meeting at the junction has a special orientation, i.e., a high degree of coherency because of lattice coincidence or a rational orientation (low Miller indices), the configuration is symmetric (Fig. 3) and the angles between the LAGB and both HAGBs α and α' are identical. In this case, the dihedral angle β facing the LAGB reflects the relative magnitudes of the grain boundary energies. Modifying Eq. (1) yields:

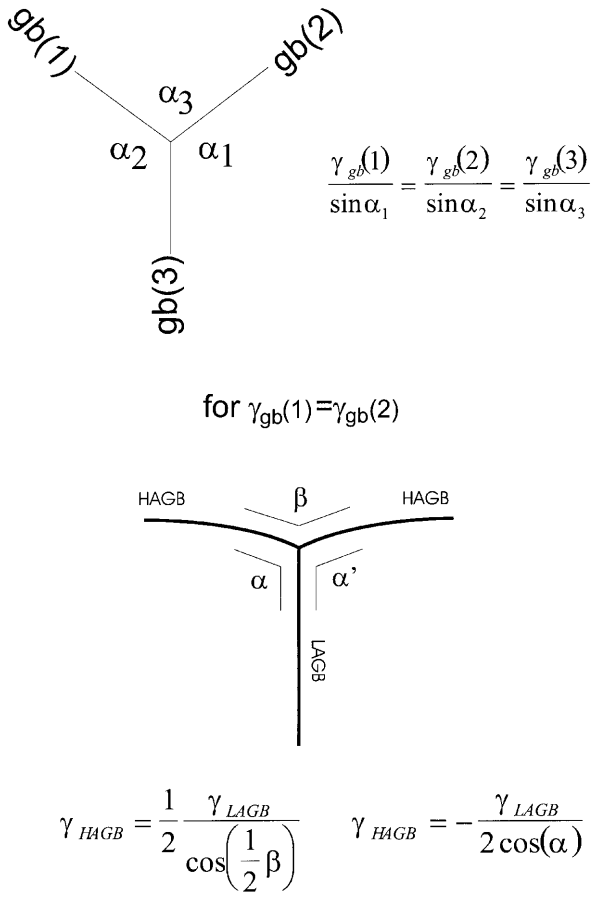

Fig. 3 Relation between boundary energies and dihedral angles

$$\gamma_{\mathrm{HAGB}} = \frac{1}{2}\frac{\gamma_{\mathrm{LAGB}}}{\cos\left(\frac{1}{2}\beta\right)} \tag{2}$$

Because a LAGB has a lower interfacial energy than a general HAGB, the dihedral angle β exceeds 120°. If an absolute value for the energy of the LAGB can be determined, the energy of the HAGB can be calculated using Eq. (2).

The variation of interfacial free energy with the orientation of the interface

The above holds, if the grain boundary energy is independent of its orientation with respect to the lattice of one or both adjoining crystals. For those cases where a grain boundary can lower its energy by moving into a special orientation (i.e., an orientation with low Millers indices) an extra force must be applied to keep the grain boundary out of the special orientation. In such a case the angles α and α' are not identical. The forces that pull the grain boundary into a special orientation are termed torque forces (Kelly and Groves 1970; Sutton and Baluffi 1996). Adding torque forces of unknown magnitude to the equilibrium of forces in Eq. (1) gives a set of three equations that cannot be solved (Herring 1951).

Faceted interphase boundaries between olivine and basaltic melt have been observed in melting experiments by numerous authors (Riley and Kohlstedt 1991; Faul 1997; Cmiral et al. 1998; Jung and Waff 1998), and are taken to indicate anisotropic phase boundary energies. However, the HAGB in the sample investigated in this study are not faceted (Fig. 1d–f). Thus, their orientation cannot be influenced significantly by torque forces. It is concluded that in our case the torque forces exerted on HAGB are so small that they can be ignored. In contrast, the LAGB generally reveal a special orientation parallel to (100) (Figs. 1a, b and 2a, b). Because this special orientation is obviously a low energy configuration, there are no torque forces that attempt to move the LAGB out of this position, and torque forces acting on the LAGB can be taken as zero. In this case, the set of equations of Herring (1951) can be solved.

Figure 2a shows the typical configuration of grain boundaries, as seen in the optical microscope. Even though the boundaries are not perfectly smooth, the error encountered when measuring the dihedral angle is estimated to $<1°$ and the distortion of the HAGB caused by torque forces must be negligibly small in comparison with the effects of the grain boundary tension of the LAGB. Occasionally, deviations from this expected pattern occur. They are suspected to result from impurity drag or pinning at phase boundaries not visible within the volume of the thin section.

Balancing the forces parallel to the LAGB gives:

$$\gamma_{LAGB} = -\gamma_{HAGB}\cos\alpha - \gamma_{HAGB}\cos\alpha' + (T_1\cos\alpha - T_2\cos\alpha') \tag{3}$$

as visualized in Fig. 4. T_1 and T_2 denote the torque forces acting on the high-angle grain boundary. For T_1 and T_2, being so small quantities that they can be ignored, Eq. (4) simplifies to:

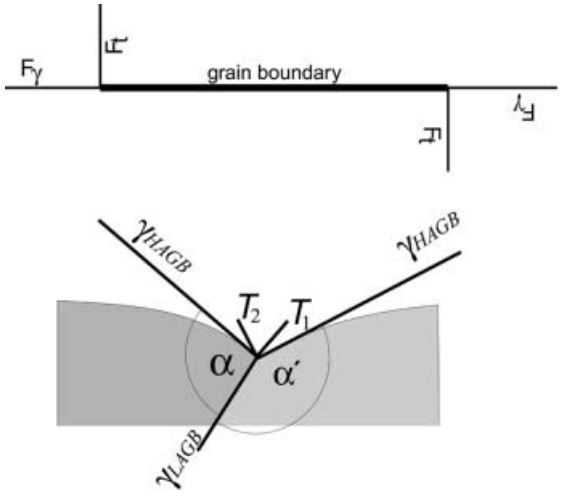

Fig. 4 Scheme visualizing the torque forces exerted on a grain boundary at a triple junction

$$\gamma_{HAGB} = \frac{\gamma_{LAGB}}{\cos\alpha + \cos\alpha'} \quad (4)$$

After measuring α and α with the universal stage, γ_{HAGB} can be computed as described in the next section.

Computation of low-angle grain boundary energies from disorientation

The energy of a LAGB can be calculated following Read and Shockley (1950). These authors have proposed that the energy of an LAGB is the sum of the elastic strain energy stored around the geometrically necessary dislocations in the boundary and the so-called core energy of these dislocations. The core energy mainly represents the energy of the broken bonds along the dislocation line. The core can be understood as the volume of crystal around a dislocation line, which is distorted so much that the laws of elasticity no longer apply. A rough estimate of the core energy is provided by the energy of fusion (Bollmann 1970). For simplification, Read and Shockley (1950) introduced a core radius r_o. This is defined in such a way that an integration of the elastic energy down to the core radius r_o gives the total energy of the dislocation, including the core energy. Principally, the core energy and, therefore, the core radius r_o are unknown. High core energies imply small core radii, and vice versa.

The dislocations forming an LAGB can be of screw type or of edge type. The types of dislocations building up an LAGB and their Burgers vectors can be determined from the orientation of the rotation axis with respect to the grain boundary plane (Frank 1950; Bilby 1955). The energy of edge dislocations is higher by a factor of $1/(1–v)$ compared with screw dislocations, where v denotes the Poisson ratio.

The tilt boundaries identified in most of the investigated olivine grains are made up of a regular configuration of edge dislocations parallel to one other. Unilaterally, rational LAGBs parallel to (100) of one of the bordering sub-grains predominate, with the rotation axis near [001]. For this configuration, the Burgers vector **b** of the geometrically necessary dislocations is parallel to [100] and perpendicular to the sub-grain boundary. The dislocation lines are parallel to [001], slip has taken place on (010) planes. Because the boundary is not symmetric, some few additionally dislocations with Burgers vector [010] are geometrically necessary Following Read (1953), the energy of symmetrical sub-grain boundaries can be calculated as follows. The spacing between the dislocation lines h depends on the length b of the Burgers vector and the tilt angle θ as follows:

$$h = b/(tan\theta))$$

or for low angles

$$h \approx b/\theta \quad (6)$$

Then, following Read and Shockley (1950), the energy of a low angle tilt boundary per unit area as a function of disorientation is

$$\gamma_{LAGB} = Eo\theta(Ao - ln\theta) \quad (7)$$

where

$$Eo = Gb/(4\pi(1-v))$$

and

$$\mathrm{A}o = 1 + ln\left(\frac{b}{2\pi r0}\right)$$

where G is the shear modulus, v is Poisson's ratio and r_o the core radius.

If the LAGB is asymmetric, additional dislocations with a Burgers vector perpendicular to that of the predominating dislocation type are geometrically necessary (Read 1953). Eo and Ao change to

$$\begin{aligned} Eo &= \tfrac{Gb}{4\pi(1-v)}(\cos\chi + \sin|\chi|) \\ Ao &= 1 + \ln\left(\tfrac{b}{2\pi r_0}\right) - \tfrac{1}{2}\sin 2|\chi| \\ &\quad - \frac{\sin|\chi|\ln(\sin|\chi|) + \cos\chi\ln(\cos\chi)}{\sin|\chi| + \cos\chi} \quad B > I > /I > /B > \end{aligned} \quad (8)$$

with χ denoting the angle between the interface and the bisecting plane for both lattice orientations. For a unilaterally rational tilt boundary χ equals /2. This relationship suggests that asymmetric tilt boundaries should reveal higher energies than symmetric tilt boundaries. Note that Eq. (8) is valid for the cubic case only because, in olivine, the Burgers vector parallel to [010] is more than twice as long as the Burgers vector parallel to [100].

The above equations do not include anisotropy in the energy calculations. The term E_0 in Eq. (7) contains the isotropic elastic parameters shear modulus G and Poisson's ratio v. For straight dislocations in anisotropic elastic media the term $G/(1–v)$ in E_0 can be replaced by an energy factor K (Eshelby et al. 1953). Following the formalism outlined by Hirth and Lothe (1992) we calculated K from the elastic stiffnesses. E_0 in Eq. (7) then becomes

$$E_0 = \frac{Kb}{4\pi} \ .$$

Grain boundary configuration in olivine

In our specimen, the HAGBs are not facetted. Short segments of plane HAGBs with switches in orientation on the order of 5°, which can be observed occasionally, are interpreted to reflect pinning by impurities or junctions with other interfaces outside the volume of the thin section, rather than reflecting a low energy position. In contrast, the LAGBs are predominantly unilaterally

rational tilt boundaries parallel to (100) with a rotation axis near [001]. In places, LAGBs parallel to (001) with a rotation axis near [100] also occur. The first type indicates that slip took place on the (010) planes in the [100] direction, the second type indicates slip on the (010) planes in [001] direction. Both slip systems are activated at high temperatures (Nicolas and Poirier 1976).

LAGBs parallel to (100) generally retain a constant orientation when approaching a HAGB at an oblique angle, even though a change in orientation of the LAGB would decrease the boundary area. Figure 2a shows four sub-grains with different disorientations and the respective crystallographic and grain boundary orientations. All LAGB are parallel to (100) of one of the sub-grains, with the rotation axis close to (100). The dihedral angle facing the sub-grains systematically decreases with increasing disorientation. Figure 2b shows an LAGB that is rational with respect to one of the sub-grains for most of its length, and then becomes rational with respect to the other sub-grain close to the grain edge.

Occasionally, low-angle grain boundaries parallel to (010) were observed, that changed their orientation and became curved near the grain edge. In these cases the angle between HAGB and LAGB is so small that the free energy gained by shortening of the interface results in forces large enough to pull the grain boundary out of the rational position.

For the grain edges fulfilling all above criteria, with (100) LAGB meeting two general HAGBs, the sub-grain disorientation is plotted against the relative grain boundary energy derived from dihedral angles in Fig. 5.

According to Eqs. (7) and (8), the energy of asymmetric low-angle tilt boundaries is expected to exceed those of symmetric tilt boundaries with identical disorientation by a few percent. This is probably not true for olivine, as indicated by the predominance of asymmetric, unilaterally rational LAGBs. Therefore, we believe that the application of the simpler Read and Shockley (1950) formula for symmetric low-angle tilt boundaries to the asymmetric case is justified. In any case, the predicted difference of a few percent remains within the limits of error inherent in the measurements.

Elastic stiffnesses for olivine of similar composition and their pressure and temperature derivatives were reported by Kumazawa and Anderson (1969) and Zha et al. (1998). Temperature- and pressure-compensated values of the anisotropic energy factor K for a dislocation line parallel to [001] and a Burgers vector [100] were calculated from these data as

$$K = 103.2\,\text{GPa}, |\mathbf{b}_{[100]}| = 4.76 \times 10^{-10}\text{mm}$$

at 800 °C and 1 GPa, and

$$mK = 104.3\,\text{GPa}, |\mathbf{b}_{[100]}| = 4.75 \times 10^{-10}\text{mm}$$

at 1000 °C and 2 GPa.

These data show that, in our case, including the effects of anisotropy in the Read and Shockley equations does not significantly influence the results. For edge dislocations parallel [001] with a Burgers vector [100], K is quite close to the isotropic value of $G/(1-\nu)$, when G and ν are calculated from the Voigt averages of the stiffnesses (102.9 and 104.0 GPa). Because K enters the energy equation as a linear factor, the dependence of K on temperature and pressure is negligible.

In order to obtain the desired absolute values for the LAGB energies, and then that of the HAGBs from the dihedral angles, the core energy of the dislocations must first be determined. Choosing an inappropriate r_o has a strong effect on the computed energies for LAGB if the disorientation θ exceeds a few degrees. Cooper and Kohlstedt (1982) have estimated r_o as 1/4b. Because in our study the disorientations are significantly higher than those studied by Cooper and Kohlstedt, we have checked the validity of this core radius as follows. Varying r_o yields different shapes of the function of boundary energy versus disorientation (Fig. 6), as defined by Eq. (7). From this set of functions we have

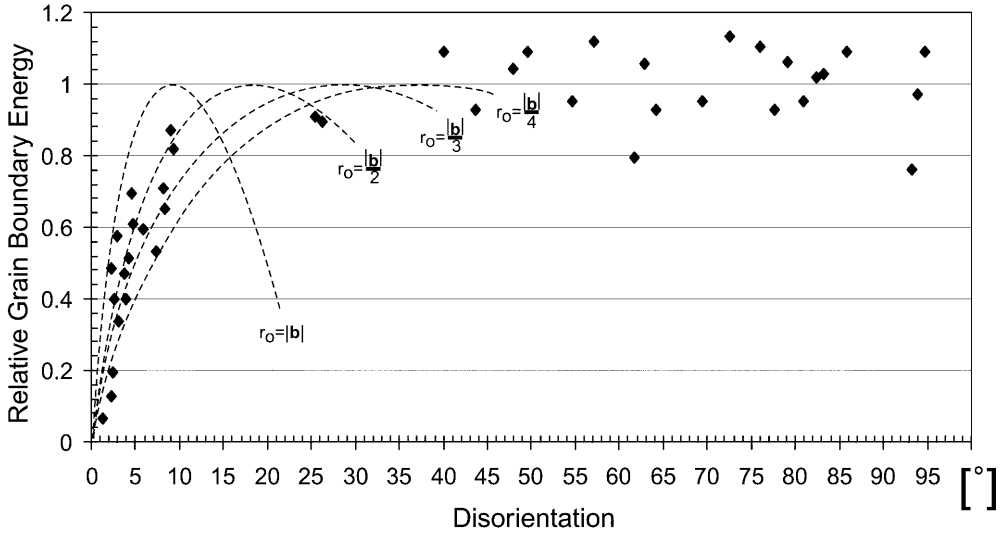

Fig. 5 Relative energies of low- to high-angle grain boundaries in olivine determined from the dihedral angles. The theoretical curves of LAGB energies as a function of disorientation after Read and Shockley (1950) are plotted for different r_o, and scaled to a maximum value of unity

chosen the one that most closely fits the relative energy vs θ plot obtained for our sample for disorientations up to 10°. The best fit suggests a core radius of 1/2b. For this core radius, the value of a high-angle grain boundary energy in olivine is ~1.4 J m^{-2} at 1000 °C and pressures of 1–2 GPa.

Absolute values of HAGB IFE are displayed in Fig. 7 computed for four different values of r_o and plotted against the disorientation at the LAGB from which the HAGB energy was determined. In the ideal case, a single IFE would be expected within one diagram. Using an inappropriate r_o results in dipping trend-lines. The best fit is achieved for an r_o of b/2.

Using the core radius of 1/4b results in computed LAGB energies of >1 N m^{-2} at only 5° disorientation (Fig. 6). Dihedral angles facing LAGB of this disorientation indicate that the energies of these LAGB are still considerably smaller than those of general large angle grain boundaries. Therefore, the core radius used by Cooper and Kohlstedt is not consistent with the HAGB IFE of 0.9 ± 0.35 J m^{-2} reported by these authors.

Discussion and conclusions

The absolute value for the energy of a general HAGB depends on the LAGB energy obtained from the dislocation model. The Read and Shockley (1950) model predicts that a symmetrical LAGB should be energetically favorable. In contrast, our analysis has revealed that unilaterally rational tilt LAGBs parallel to (100) predominate. Thus, the dislocation model based on Read and Shockley (1950) may be too simplistic for application to silicates. However, according to the Read and Shockley model, the IFE of unilaterally rational LAGBs is predicted to exceed that of symmetrical LAGBs of identical disorientation by only a few percent. This is well within the limits of error inherent in the methods applied in this study, and thus the application

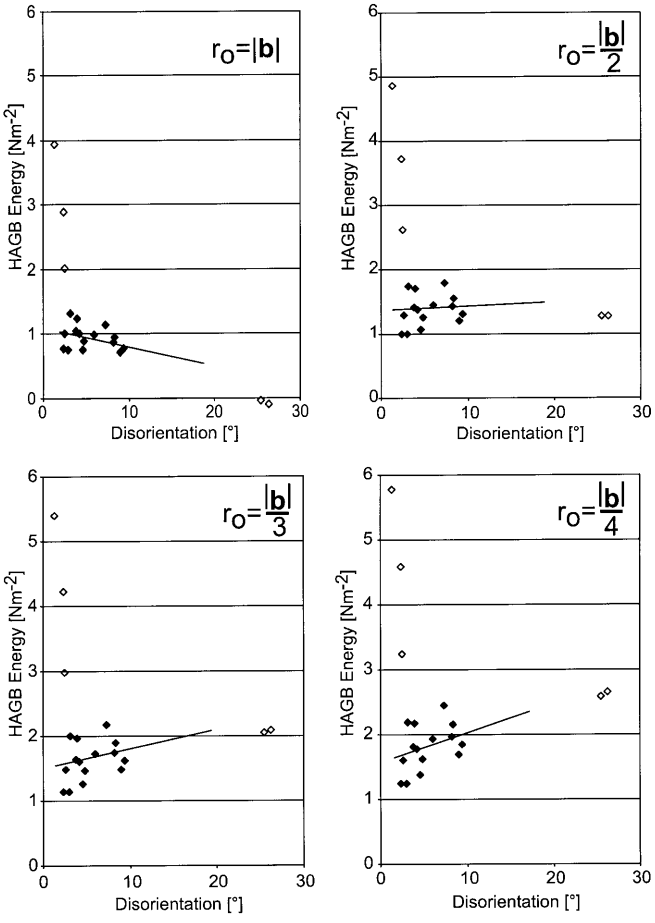

Fig. 7 Absolute values of HAGB IFE computed from LAGB IFE and different disorientations. The relation between LAGB and HAGB energies is derived from the dihedral angles. Absolute LAGB IFE were calculated for different r_o. A nearly identical value for the HAGB should be obtained for all disorientations. Inclined trend lines (fitted by least square errors) indicate inappropriately chosen r_o. The best fit is achieved for $r_o = b/2$. Only the *filled data points* were used for the line fitting. Note that at disorientation angles below 1.5° the IFE versus disorientation curve is very steep, resulting in large errors in the HAGB energy calculation

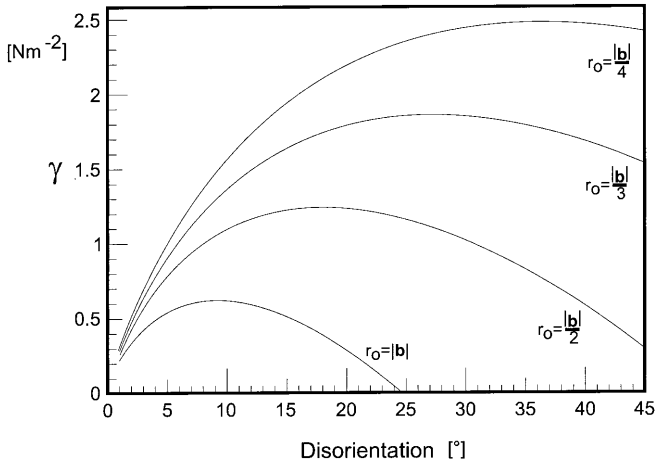

Fig. 6 Variation of the grain boundary energy γ of low-angle grain boundaries as a function of disorientation and core radius r_o according to the formula of Read and Shockley (1950)

of the Read and Shockley model for symmetrical LAGBs appears to be justified. The model successfully predicts grain boundary energies as a function of disorientation for metals, e.g., Dhalenne et al. (1982), Mori et al. (1988), Otsuki et al. (1988), and Wolf (1989). Also, the plot of LAGB disorientation versus relative IFE for olivine, as derived from dihedral angles, corresponds to the Read and Shockley function for a core radius of 1/2 |**b**| (**b** = Burgers vector).

The derived absolute IFE value for HAGBs is influenced by the presumed conditions prevailing at the time when the IFE-controlled grain-boundary configuration is adjusted, because both elastic moduli and length of the Burgers vector depend on temperature and pressure. The value of 1.4 ± 0.4 J m^{-2} holds for a temperature ~1,000 °C and pressures of 1–2 GPa.

Our value compares favorably with the 0.9 ± 35 J m^{-2} value obtained by Cooper and Kohlstedt (1982) in

their experimental study with melt present. The conditions of Cooper's and Kohlstedt's experiments (1600 °C and 1 atmosphere) result in the anisotropic energy term K in Eq. (7) being ~10% lower, resulting in 10% lower IFE.

The use of natural materials has the following advantages:

1. No experimental efforts – besides thin section preparation – are required.
2. The material is coarse-grained and thus three-dimensional grain boundary configuration and crystallographic orientation can be studied simultaneously in transmitted light. This is not possible for fine-grained material studied with the scanning electron microscope.
3. The low energy grain boundary configuration was adjusted over geological time scales in the solid state.
4. Potential effects of impurities are those relevant to natural conditions.

It is anticipated that the combination of classical transmitted light microscopy (to specify interface configurations in three dimensions) with electron backscatter diffraction techniques (EBSD) to quantify disorientation, will allow for similar studies on single and polyphase aggregates in natural rocks, and thus contribute to an improved understanding of the properties of interfaces in geological materials.

Acknowledgements Thanks are due to Olaf Medenbach for his help with the determination of the refractive indices. Stuart Thomson kindly improved the English. The constructive reviews of Martyn Drury and an anonymous reviewer helped to improve the manuscript. Financial support for parts of this study from the German Science Foundation within the scope of the Collaborative Research Center (SFB 526) "Rheology of the Earth – from the upper crust into the subduction zone" is gratefully acknowledged.

References

Bilby BA (1955) Report on the conference on defects in crystalline solids. The Physical Society, London, p 123
Bollmann W (1970) Crystal defects and crystalline interfaces. Springer, Berlin Heidelberg New York
Bulau JR, Waff HS, Tyburczy JA (1979) Mechanical and thermodynamic constraints of fluid distribution in partial melts. J Geophys Res 84: 6102–6108
Cmiral M, Gerald JDF, Faul UH, Green DH (1998) A close look at dihedral angles and melt geometry in olivine-basalt aggregates: a TEM study. Contrib Mineral Petrol 130: 336–345
Coltorti M, Siena F (1984) Mantle tectonite and fractionate periodotite at Finero (Italian Western Alps). N Jahrb Mineral Abh 149(3): 255–244
Cooper RP, Kohlstedt DL (1982) Interfacial energies in the olivine–basalt system: In: Akimoto S, Manghnani MH (eds) Advances in Earth and planetary sciences, vol 12: High pressure research in geophysics. Center for Academic Publication, Tokyo, pp 217–228
Dhalenne G, Dechamps M, Revcolevschi A (1982) Relative energies of tilt boundaries in NiO. J Am Ceram Soc 65: C/11–12
Eshelby JD, Read WT, Shockley W (1953) Anisotropic elasticity with applications to dislocation theory. Acta Metal 1: 251
Faul H (1997) Permeability of partially molten upper mantle rocks from experiments and percolation theory. J Geophys Res B102: 10299–10311
Frank FC (1950) Symposium on the plastic deformation of crystalline solids. Office of Naval Research, Pittsburg, Pennsylvania, p 150
Herring C (1951) The physics of powder metallurgy. McGraw Hill, New York
Hirth JP, Lothe J (1992) Theory of dislocations. Krieger, Malabar
Jung H, Waff HS (1998) Olivine crystallographic control and anisotropic melt distribution in ultramafic partial melts. Geophys Res Lett 25(15): 2901–2904
Kelly A, Groves GW (1970) Crystallography and crystal defects. Longman, London
Kretz R (1966) Interpretation of the shape of mineral grains in metamorphic rocks. J Petrol 7(1): 68–94
Kretz R (1969) On the spatial distribution of crystals in rocks. Lithos 2: 39–65
Kruhl JH, Voll G (1979) Deformation and metamorphism of the western Finero Complex. Mem Ist Geol Minerol Univ Padova 33: 95–109
Kumazawa M, Anderson OL (1969) Elastic moduli, pressure derivatives, and temperature derivatives of single crystal olivine and single crystal forsterite. J Geophys Res 74: 5961–5972
Lensch G (1968) Die Ultramafitite der Zone von Ivrea und ihre geologische Interpretation. Schweiz Mineral Petrogr Mitt 48(1): 91–102
Lu MH, Hofman AW, Mazzuchelli M, Rivalenti G (1997a) The mafic–ultramafic complex near Finero (Ivrea–Verbano-Zone). 1. Chemistry of MORB like magmas. Chem Geol 140(3–4): 207–222
Lu MH, Hofman AW, Mazzuchelli M, Rivalenti G (1997b) The mafic–ultramafic complex near Finero (Ivrea–Verbano-Zone). 2. Geochronology and isotope geochemistry. Chem Geol 140(3–4): 223–235
Mori T, Miura H, Tokita T, Haji J, Kato M (1988) Determination of the energies of (001) twist boundaries in Cu with the shape of boundary SiO/sub 2/ particles. Phil Mag Lett 58: 11–15
Murr LE (1975) Interfacial phenomena in metals and alloys. Addison–Wesley, London
Nicolas A, Poirier JP (1976) Crystalline plasticity and solid state flow in metamorphic rocks. Wiley, London, pp 171–183
Otsuki A, Isono H, Mizuno M (1988) Energy and structure of (100) aluminium grain boundary. J Phys Colloq 49(C-5): 563–568
Read WT (1953) Dislocations in crystals. McGraw Hill, New York
Read WT, Shockley W (1950) Dislocation models of crystal grain boundaries. Phys Rev 78(3): 275–289
Riley GNJr, Kohlstedt DL (1991) Kinetics of melt migration in upper mantle-type rocks. Earth Planet Sci Lett105: 500–521
Smith CS (1964) Some elementary principles of polycrystalline microstructures. Metal Rev 9: 1–48
Spry A (1969) Metamorphic textures. Pergamon, Oxford
Sutton AP, Baluffi RW (1996) Interfaces in crystalline materials. Monograph Phys Chem Materials no 51. Clarendon, Oxford
t'Hart J (1978a) The structural morphology of olivine. II. A quantitative derivation. Can Mineral 16: 547–560
t'Hart J (1978b) The structural morphology of olivine. I. A qualitative derivation. Can Mineral 16: 547–560
Turamori A, Fujii N (1986) Connectivity of melt phase in a partially molten peridotite. J Geophys Res 84: 9239–9252
Vernon RH (1976) Metamorphic processes. Allen and Unwin, London
Voll G (1960) New work on petrofabrics. Liverpool and Manchester. Geol J 2(3): 503–567
Underwood EE (1970) Quantitative stereology. Addison-Wesley, Reading
Waff HS, Bulau JR (1979) Equilibrium fluid distribution in an ultramafic partial melt under hydrostatic stress conditions. J Geophys Res 84: 6109–6114
Waff HS, Bulau JR (1982) Experimental determination of near equilibrium textures in partially molten silicates at high pressures. In: Akimoto S, Manghnani MH (eds) Advances in Earth and planetary sciences, vol 12. High pressure research in

geophysics. Center for Academic Publication, Tokyo, pp 229–236
Waff HS, Faul UH (1992) Effects of crystalline anisotropy on fluid distribution in ultramafic partial melts. J Geophys Res 97: 9003–9014
Wolf D (1989) A Read–Shockley model for high-angle grain boundaries. Scr Metal 23: 1713–1718
Zanetti A, Mazzucchelli M, Rivalenti G, Vannucci R (1999) The Finero phlogopite-peridotite massif: an example of subduction-related metasomatism. Contrib Mineral Petrol 134(2/3): 107–122
Zha CS, Duffy TS, Downs RT, Mao HK, Hemley RJ (1998) Brillouin scattering and X-ray diffraction of San Carlos olivine: direct pressure determination to 32 GPA. Earth Planet Sci Lett 159: 25–33
Zingg A (1983) The Ivrea and Strona-Ceneri zones (Southern Alps, Ticino and N-Italy); a review. Schweizer Miner Petrogr Mitt 63(2–3): 361–392